VIRAL PALEOGENOMICS

Ancient chicken remains reveal the origins of virulence in Marek's disease virus

Steven R. Fiddaman[1]*†, Evangelos A. Dimopoulos[2,3]†, Ophélie Lebrasseur[4,5], Louis du Plessis[6,7], Bram Vrancken[8,9], Sophy Charlton[2,10], Ashleigh F. Haruda[2], Kristina Tabbada[2], Patrik G. Flammer[1], Stefan Dascalu[1], Nemanja Marković[11], Hannah Li[12], Gabrielle Franklin[13], Robert Symmons[14], Henriette Baron[15], László Daróczi-Szabó[16], Dilyara N. Shaymuratova[17], Igor V. Askeyev[17], Olivier Putelat[18], Maria Sana[19], Hossein Davoudi[20], Homa Fathi[20], Amir Saed Mucheshi[21], Ali Akbar Vahdati[22], Liangren Zhang[23], Alison Foster[24], Naomi Sykes[25], Gabrielle Cass Baumberg[2], Jelena Bulatović[26], Arthur O. Askeyev[17], Oleg V. Askeyev[17], Marjan Mashkour[20,27], Oliver G. Pybus[1,28], Venugopal Nair[1,29], Greger Larson[2]‡, Adrian L. Smith[1]*‡, Laurent A. F. Frantz[30,31]*‡

The pronounced growth in livestock populations since the 1950s has altered the epidemiological and evolutionary trajectory of their associated pathogens. For example, Marek's disease virus (MDV), which causes lymphoid tumors in chickens, has experienced a marked increase in virulence over the past century. Today, MDV infections kill >90% of unvaccinated birds, and controlling it costs more than US$1 billion annually. By sequencing MDV genomes derived from archeological chickens, we demonstrate that it has been circulating for at least 1000 years. We functionally tested the *Meq* oncogene, one of 49 viral genes positively selected in modern strains, demonstrating that ancient MDV was likely incapable of driving tumor formation. Our results demonstrate the power of ancient DNA approaches to trace the molecular basis of virulence in economically relevant pathogens.

Marek's disease virus (MDV) is a highly contagious alphaherpesvirus that causes a tumor-associated disease in poultry. At the time of its initial description in 1907, Marek's disease was a relatively mild disease with low mortality, characterized by nerve pathology that affected mainly older individuals (*1*). However, over the course of the 20th century, MDV-related mortality has risen to >90% in unvaccinated chickens. To prevent this high mortality rate, the poultry industry spends more than US$1 billion per year on health intervention measures, including vaccination (*2*).

The increase in virulence and clinical pathology of MDV infection has likely been driven by a combination of factors. First, the growth in the global chicken population since the 1950s led to more viral replication, which increased the supply of new mutations in the population. In addition, the use of imperfect (also known as "leaky") vaccines that prevent symptomatic disease but do not prevent transmission of the virus likely shifted selective pressures and led to an accelerated rate of MDV virulence evolution (*3*). Combined, these factors have altered the evolutionary trajectory, resulting in modern hyperpathogenic strains. To date, the earliest sequenced MDV genomes were sampled in the 1960s (*4*), several decades after the first reports of MDV causing tumors (*5*). As a result, the genetic changes that contributed to the increase in virulence of MDV infection before the 1960s remain unknown.

MDV has been circulating in Europe for at least 1000 years

To empirically track the evolutionary change in MDV virulence through time, we generated MDV genome sequences (serotype 1) isolated from the skeletal remains of archeological chickens. We first shotgun sequenced 995 archeological chicken samples excavated from more than 140 western Eurasian archeological sites and screened for MDV reads using HAYSTAC (*6*) with a herpesvirus-specific database. Samples with any evidence of MDV reads were then enriched for viral DNA by using a hybridization-based capture approach based on RNA baits designed to tile the entire MDV genome (excluding one copy of each of the terminal repeats and regions of low complexity). To validate the approach, we also captured and sequenced DNA from the feather of a modern Silkie chicken that presented MDV symptoms. As a negative control, we also included an ancient sample that displayed no evidence of MDV reads after screening (OL1214; Serbia, 14th to 15th century).

Using the capture protocol, we identified 15 ancient chickens with MDV-specific reads of ≥25 base pairs (bp) in length. This approach also yielded a ~4× genome from a modern positive control. We found that the majority (88 to 99%) of uniquely mapped reads that were generated from ancient samples classified as MDV-positive were ≥25 bp, whereas the majority (53 to 100%) of uniquely mapped reads that were generated from samples considered MDV-negative were <25 bp. In addition, samples considered MDV-positive yielded between 308 and 133,885 uniquely mapped reads (≥25 bp), whereas samples considered MDV-negative (including a negative control) (table S2) yielded between 0 and 211 uniquely mapped reads of ≥25 bp. MDV-positive ancient samples ranged in depth of coverage from 0.13× to 41.92× (OL1385) (Fig. 1A and table S2), with seven genomes at ≥2× coverage.

In all positive samples, the proportion of duplicated reads approached 100%, which indicated that almost all of the molecules in each library were sequenced at least once (fig. S1). Reads obtained from MDV-positive ancient samples had chemical signatures of DNA damage typically associated with ancient DNA (fig. S2). By contrast, reads obtained from our modern positive control did not show any evidence of DNA damage (fig. S2). The earliest unequivocally MDV-positive sample (with 4760 postcapture reads ≥25 bp) was derived from a 10th- to 12th-century chicken from eastern France (Andlau in Fig. 1A and table S2). Together, these results demonstrate that MDV strains have been circulating in western Eurasian poultry for at least 1000 years.

[1]Department of Biology, University of Oxford, Oxford, UK. [2]The Palaeogenomics and Bio-Archaeology Research Network, Research Laboratory for Archaeology and History of Art, University of Oxford, Oxford, UK. [3]Department of Veterinary Medicine, University of Cambridge, Cambridge, UK. [4]Centre d'Anthropobiologie et de Génomique de Toulouse, CNRS/Université Toulouse III Paul Sabatier, Toulouse, France. [5]Instituto Nacional de Antropología y Pensamiento Latinoamericano, Ciudad Autónoma de Buenos Aires, Buenos Aires, Argentina. [6]Department of Biosystems Science and Engineering, ETH Zurich, Basel, Switzerland. [7]Swiss Institute of Bioinformatics, Lausanne, Switzerland. [8]Department of Microbiology, Immunology and Transplantation, Rega Institute, KU Leuven, Leuven, Belgium. [9]Spatial Epidemiology Lab (SpELL), Université Libre de Bruxelles, Brussels, Belgium. [10]BioArCh, Department of Archaeology, University of York, York, UK. [11]Institute of Archaeology, Belgrade, Serbia. [12]Institute of Immunity and Transplantation, University College London, London, UK. [13]Silkie Club of Great Britain, Charing, UK. [14]Fishbourne Roman Palace, Fishbourne, UK. [15]Leibniz-Zentrum für Archäologie, Mainz, Germany. [16]Medieval Department, Budapest History Museum, Budapest, Hungary. [17]Laboratory of Biomonitoring, The Institute of Problems in Ecology and Mineral Wealth, Tatarstan Academy of Sciences, Kazan, Russia. [18]Archéologie Alsace–PAIR, Sélestat, Bas-Rhin, France. [19]Departament de Prehistòria, Universitat Autònoma de Barcelona, Barcelona, Spain. [20]Bioarchaeology Laboratory, Central Laboratory, University of Tehran, Tehran, Iran. [21]Department of Art and Architecture, Payame Noor University (PNU), Tehran, Iran. [22]Iranian Ministry of Cultural Heritage, Tourism, and Handicrafts, North Khorasan Office, Iran. [23]Department of Archaeology, School of History, Nanjing University, China. [24]Headland Archaeology, Edinburgh, UK. [25]Department of Archaeology, University of Exeter, Exeter, UK. [26]Department of Historical Studies, University of Gothenburg, Gothenburg, Sweden. [27]CNRS, National Museum Natural History Paris, Paris, France. [28]Department of Pathobiology and Population Sciences, Royal Veterinary College, London, UK. [29]Viral Oncogenesis Group, Pirbright Institute, Woking, UK. [30]Palaeogenomics Group, Institute of Palaeoanatomy, Domestication Research and the History of Veterinary Medicine, Ludwig-Maximilians-Universitat, Munich, Germany. [31]School of Biological and Chemical Sciences, Queen Mary University of London, London, UK.

***Corresponding author. Email: steven.fiddaman@biology.ox.ac.uk (S.R.F.); adrian.smith@biology.ox.ac.uk (A.L.S.); laurent.frantz@lmu.de (L.A.F.F.)**

†These authors contributed equally to this work.

‡These authors contributed equally to this work.

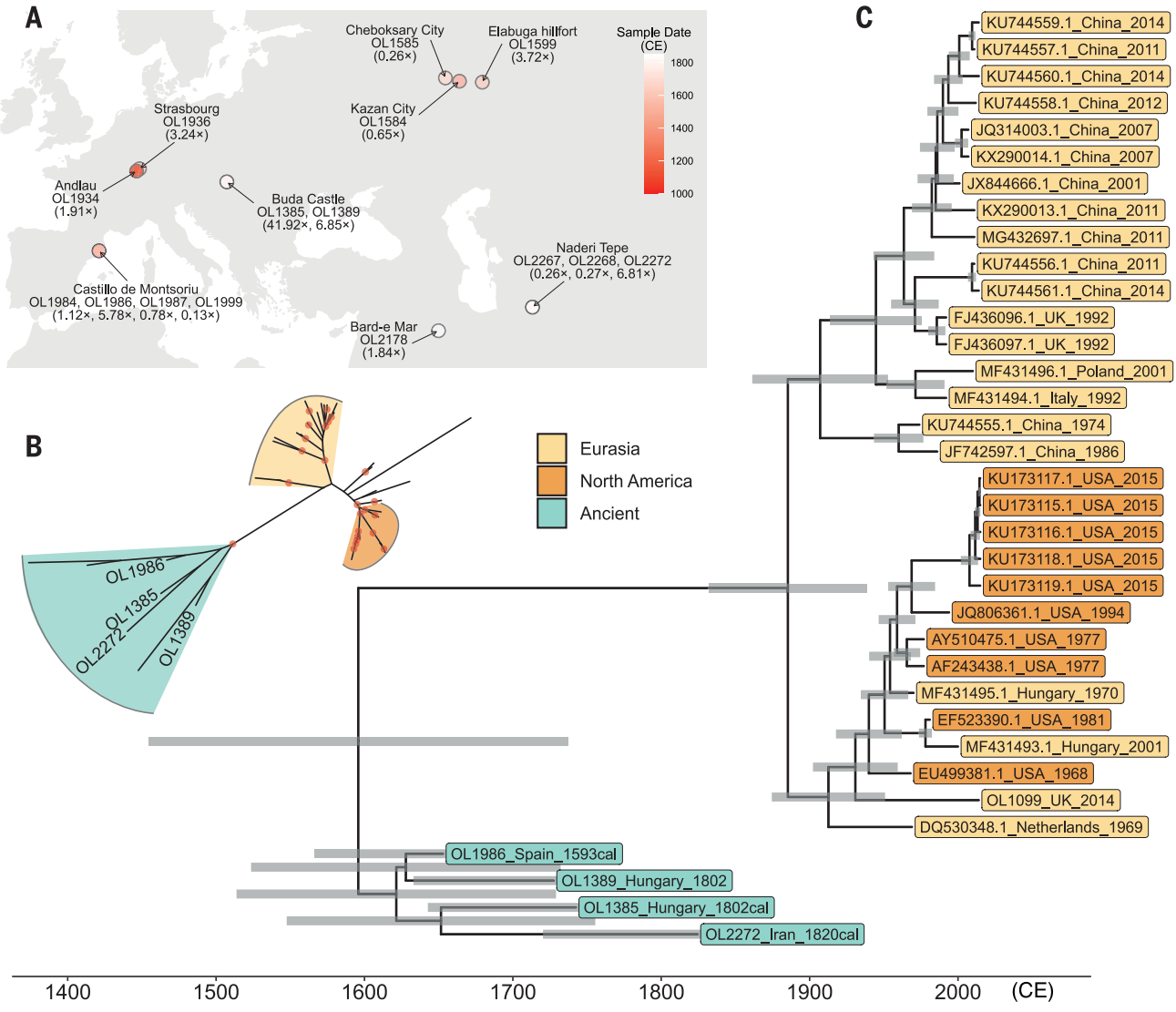

Fig. 1. Locations of MDV-positive samples and time-scaled phylogeny. (**A**) Map showing the locations of screened archeological chicken samples that were positive for MDV sequence. Colored circles indicate sample dates (either from calibrated radiocarbon dating or estimated from archeological context) (table S1). Average sequencing depth after capture is given in parentheses under sample names. If more than one sample was derived from the same site, this is indicated by a list of sample identifiers (beginning "OL") and sequencing depths in parentheses. (**B**) Unrooted NJ tree of 42 modern and 10 ancient genomes. Only the four high-coverage ancient samples used in our BEAST analysis were labeled in this tree (table S2). Nodes with bootstrap support of >90 are indicated with red dots. (**C**) Timescaled maximum clade credibility tree of ancient and modern MDV sequences by using the uncorrelated lognormally distributed (UCLD) relaxed clock and the general time-reversible (GTR) substitution model. Gray bars indicate the 95% HPD for the age of each node. The "cal" suffix for ancient samples indicates that samples were radiocarbon dated and that these date distributions were used as priors for the molecular clock analyses (*24*).

Ancient MDV strains are basal to modern lineages

To investigate the relationship between ancient and modern MDV strains, we built phylogenetic trees based on both neighbor-joining (NJ) and maximum-likelihood (ML) methods. We first built trees using 10 ancient genomes with at least 1% coverage at a depth of ≥5×, a modern positive control derived from the present study (OL1099), and 42 modern genomes from public sources (table S3). Both NJ (Fig. 1B and fig. S3) and ML trees (fig. S4) match the previously described general topology (*7*), in which Eurasian and North American lineages were evident, along with a well-supported (bootstrap 94) ancient clade (Fig. 1B). The same topology was also obtained when we restricted our ML analysis to include only transversion sites (fig. S5). Last, we built a tree using an outgroup (*Meleagrid herpesvirus 1*, accession NC_002641.1) to root our topology (fig. S6). We obtained a well-supported topology showing that the ancient MDV sequences form a highly supported clade that lies basal to all modern MDV strains (including the modern positive control OL1099).

Next, we built a time-calibrated phylogeny using BEAST [v. 1.10 (*8*)] that included 31 modern genomes collected since 1968 (table S3) and four ancient samples with an average depth of coverage >5× (OL1986, Castillo de Montsoriu, Spain, 1593 calibrated CE; OL1385, Buda Castle, Hungary, 1802 calibrated CE; OL1389, an additional Buda Castle sample from the same archeological context as OL1385; and OL2272, Naderi Tepe, Iran, 1820 calibrated CE) (Fig. 1A and tables S1 and S2). The time of the most recent common ancestor (TMRCA) of the phylogeny was 1602 CE [95% highest posterior

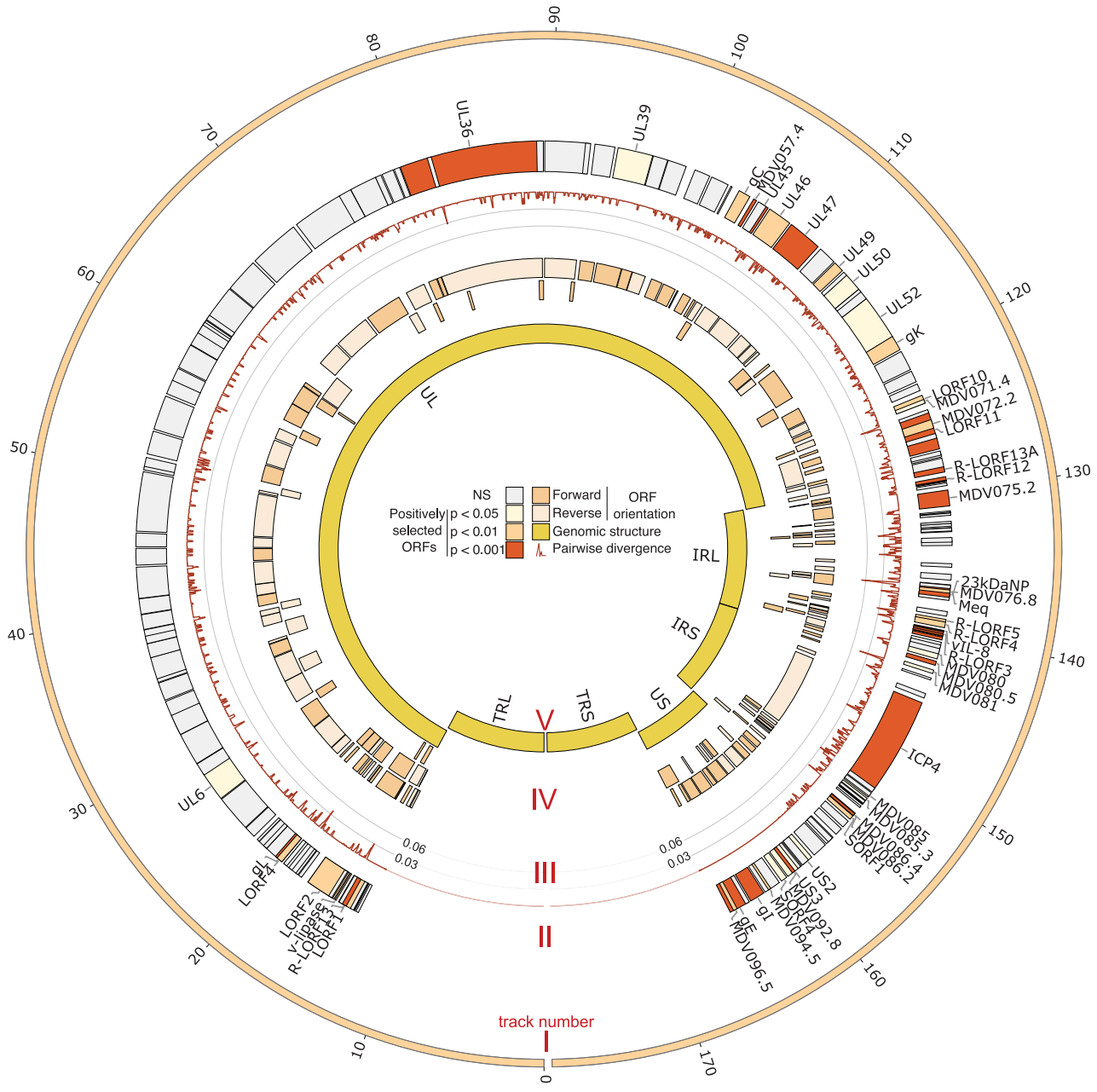

Fig. 2. Branch-site selection analysis of MDV genomes. The MDV genome is represented as a circular structure with gross genomic architecture displayed on the innermost track (track V) and genomic coordinates shown on the outermost track (units, $\times 10^3$ kb; track I). Because the long terminal repeat (TRL) and short terminal repeat (TRS) are copies of the long internal repeat (IRL) and the short internal repeat (IRS), respectively, selection analysis excluded the TRL and the TRS regions, leaving only the unique long (UL) and unique short (US) regions along with the two internal repeats. Results of the positive selection analysis are displayed on track II, where ORFs are shaded according to the strength of statistical support (corrected *P* values) for positive selection. Sliding window average pairwise divergence between ancient and modern samples is shown on track III, and ORF orientation is shown on track IV. NS, not significant.

density (HPD) interval, 1486 to 1767 CE] (Fig. 1C and table S4).

As previously reported (*7*), we found that aside from a few exceptions, most Eurasian and North American MDV strains formed distinct clades (Fig. 1B), which suggests that there has been little recent transatlantic exchange of the virus. The inclusion of time-stamped ancient MDV sequences improved the accuracy of the molecular clock analysis and pushed back the TMRCA of all modern MDV sequences, from 1922–1952 (*7*) to 1881 (95% HPD interval, 1822 to 1929) (table S4). Our mean TMRCA of modern MDV is concordant with a recent estimate that incorporated 26 modern MDV genomes from East Asian chickens [1880; 95% HPD, 1772 to 1968 (*9*)]. This phylogenetic analysis implies that the two major modern clades of MDV were likely established before the earliest documented increases in MDV virulence in the 1920s. Furthermore, because birds infected with highly virulent MDV would not have survived a transatlantic crossing, a TMRCA of 1938 (95% HPD, 1914 to 1958) for the clade containing the earliest North American sample (CU2, 1968; accession EU499381.1) could be consistent with the virus having been transmitted

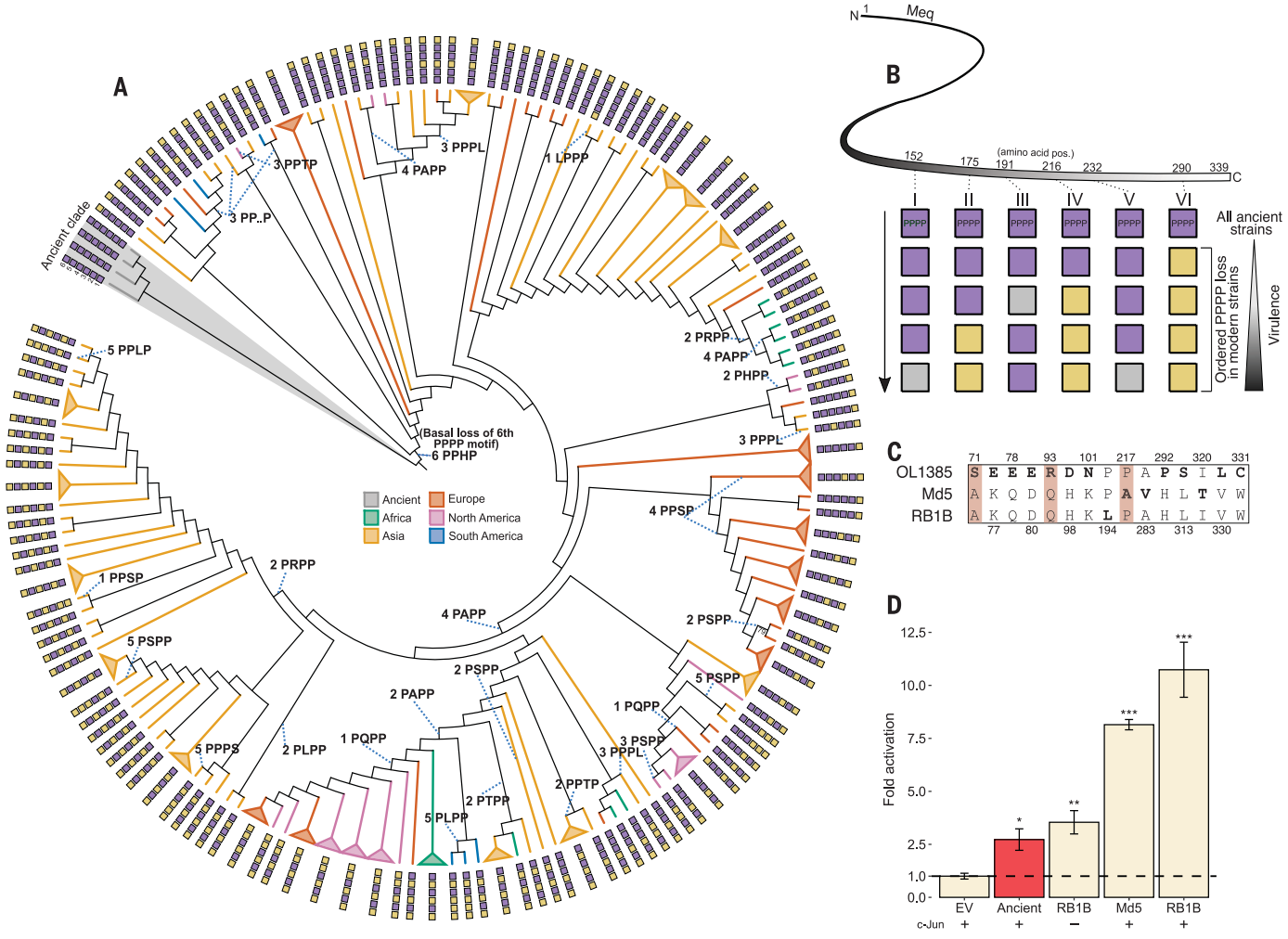

Fig. 3. *Meq* has undergone ordered loss of tetraproline repeats and increased transactivation ability. (**A**) Phylogenetic analysis of 412 *Meq* sequences of standard length (1017 bp). The outermost track shows the integrity of each tetraproline motif (purple squares, intact; yellow squares, disrupted). The mutations that disrupt the tetraproline motif are linked by dotted blue lines (for example, "4 PAPP" indicates that the fourth tetraproline motif is disrupted by a proline-to-alanine substitution in the second proline position; "3 PP..P" denotes a deletion of the third proline in the third tetraproline motif). A complete version of this figure is provided in fig. S7. A, alanine; H, histidine; L, leucine; P, proline; Q, glutamine; R, arginine; S, serine; T, threonine. (**B**) Proposed model for the most common ordered loss of tetraproline motifs in *Meq*. Purple and yellow boxes indicate presence and absence of an intact tetraproline, respectively. The gray box on the third row indicates that the third tetraproline is occasionally lost after the sixth, but typically only in terminal branches. The two gray boxes in the bottom row indicate that either the first or fifth tetraproline is lost at this point. (**C**) Positions of amino acid differences between the ancient Hungarian MDV strain (OL1385) and the two modern strains (RB1B and Md5). Positions that were also found to be under positive selection are highlighted in red. (**D**) The transactivation ability of *Meq* reconstructed from an ancient Hungarian MDV strain (OL1385) was compared with the transactivation abilities of modern strains: RB1B and Md5 (very virulent pathotypes). To show the effect of the partner protein c-Jun on transactivation ability, the strongest transactivator, RB1B, was tested with (+) and without (−) c-Jun. Transactivation ability is expressed as fold activation relative to baseline signal from an empty vector (EV). Error bars are standard deviation, and statistical significance was determined by using Dunnett's test for comparing several treatment groups with a control. *P < 0.05; **P < 0.01; ***P < 0.001.

before the most substantial virulence increases leading up to the 1960s. These results are also consistent with the hypothesis that Eurasian and North American MDV lineages independently evolved toward increased virulence (*7*).

Virulence factors are among positively selected genes in the modern MDV lineage

The rapid increase in MDV virulence could potentially have been driven by gene loss or gain, which would have substantially altered the biology of the virus (*10*, *11*). Analysis of a Hungarian, high-coverage, MDV genome (OL1385; >41×) from the 18th to 19th century indicated that it had the full complement of genes present in modern sequences. This indicates that there was no gene gain or loss in either ancient or modern lineage (Fig. 2). We also found that all MDV microRNAs, some of which are implicated in pathogenesis and oncogenesis in modern strains (*12*), were intact and highly conserved in ancient strains (table S5). Together, these results indicate that the acquisition of virulence most likely resulted not from changes in MDV genome content or organization but from point mutations.

Considering sites at which we had coverage for at least two ancient genomes, we identified 158 fixed single-nucleotide polymorphisms between the ancient and modern samples, of which 31 were found in intergenic regions and may be candidates for future study of MDV regulatory regions (table S6). To assess the impact of positive selection on point mutations,

we performed a branch-site analysis in PAML (*13*) (ancient sequences as background lineage, modern sequences as foreground lineage) on open reading frames (ORFs) using four ancient MDV genomes (OL1385, OL1389, OL1986, and OL2272). After we controlled the false discovery rate using the Benjamini-Hochberg procedure (*14*), this analysis identified 49 ORFs with significant evidence for positive selection (Fig. 2 and table S7).

Several positively selected loci identified in this analysis have previously been associated with MDV virulence in modern strains. Some of these are known immune modulators or potential targets of a protective response. This includes ICP4 (infected cell protein 4), a large transcriptional regulatory protein involved in innate immune interference. ICP4 appears to be an important target of T cell–mediated immunity against MDV in chickens that have the B21 major histocompatibility complex (MHC) haplotype (*15*), and it is plausible that sequence variation in important ICP4 epitopes could confer differential susceptibility to infection.

We also identified signatures of positive selection in several genes that encode viral glycoproteins (gC, gE, gI, gK, and gL). Glycoproteins are important targets for the immune response to MDV (*16*). Most MDV peptides presented on chicken MHC class II are derived from just four proteins (*17*), of which two were glycoproteins found to be under selection in our analysis (gE and gI). This result indicates that glycoproteins are likely under selection in MDV because they are immune targets. The limited scope of immunologically relevant MDV peptides presented by MHC class II may have important implications for vaccine development.

Positive selection was also detected in the viral chemokine termed viral interleukin-8 (vIL-8) [considered a functional ortholog of chicken CXC ligand 13 (*18*)]. vIL-8 is an important virulence factor that recruits B cells for lytic replication and $CD4^+$ $CD25^+$ T cells that are transformed to generate lymphoid tumors. Viruses that lack vIL-8 are severely impaired in the establishment of infection and generation of tumors through bird-to-bird transmission (*19*), so sequence variation in this gene could plausibly affect transmission.

The key oncogene of MDV has experienced positive selection and an ordered loss of tetraproline motifs

Our selection scan also identified Meq, a transcription factor considered to be the master regulator of tumor formation in MDV (*20*). The *Meq* coding sequence had the greatest average pairwise divergence between ancient and modern strains across the entirety of the MDV genome (Fig. 2), implying that there were numerous sequence changes along the branch that leads to modern samples. Animal experiments have demonstrated that *Meq* is essential for tumor formation (*20*), and polymorphisms in this gene, even in the absence of variants elsewhere in the genome, are known to confer substantial differences in strain virulence or vaccine breakthrough ability (*21*).

Meq exerts transcriptional control on downstream gene targets (in both the host and the viral genome) through its C-terminal transactivation domain. This domain is characterized by PPPP (tetraproline) repeats spaced throughout the second half of the protein, and the number of tetraproline repeats is inversely proportional to the virulence of the MDV strain (*22*). The difference in the number of tetraproline repeats in most strains is the result of point mutations rather than deletion or duplication; these strains are considered "standard-length" Meq (339 amino acids). In some strains, however, tetraproline repeats have been duplicated ("long" Meq strains, 399 amino acids) or deleted ("short" Meq strains, 298 amino acids; or "very short" Meq, 247 amino acids). These mutations have led to varying numbers of tetraproline repeats between strains.

We did not find any evidence of duplication or deletion in ancient Meq sequences, which indicates that these are standard-length Meq. We then identified point mutations in a database that contains four ancient Meq sequences (OL1385, OL1389, OL1986, and OL2272) along with 408 modern standard-length Meq sequences (table S8). This analysis demonstrated that ancient Meq had six intact tetraproline motifs, whereas all modern standard-length Meq sequences had between two and five. All ancient Meq sequences had a distinctive additional intact tetraproline motif at amino acids 290 to 293. This tetraproline motif was disrupted by a point mutation—causing a change from proline to histidine—in the recent evolutionary history of standard length–Meq MDV strains.

To further explore the virulence-related disruption of tetraprolines in modern *Meq* sequences, we constructed a phylogeny of *Meq* sequences (Fig. 3A). Mapping the tetraproline content of each sequence on the phylogeny indicated that tetraprolines have been lost in a specific order. After the universal disruption of the sixth tetraproline through a point mutation (at amino acids 290 to 293) at the base of the modern MDV lineage, the fourth tetraproline was disrupted at the base of two major lineages (amino acids 216 to 219). Disruption of the fourth tetraproline was followed in seven independent lineages by the disruption of the second tetraproline (amino acids 175 to 178) and then by the loss of either the first (amino acids 152 to 155) or the fifth tetraproline (amino acids 232 to 235) in six lineages (Fig. 3, A and B).

Our analysis indicated that the second and fourth tetraprolines (codons 176 and 217) were under positive selection (table S7). Although there were some observations of virus lineages that exhibited an alternative loss order [for example, the occasional loss of the third tetraproline (amino acids 191 to 194) after the loss of the fourth], such lineages are not widespread, which suggests that they may become stuck in local fitness peaks and are outcompeted by lineages following the order described here. The independent recapitulation of this pattern in different lineages suggests that loss of tetraproline motifs acts as a ratchet, in which each subsequent loss results in an increase in virulence, and once lost, motifs are unlikely to be regained.

Ancient Meq is a weak transactivator that likely did not drive tumor formation

The initial description of Marek's disease in 1907 did not mention tumors (*1*). Given the degree of sequence differentiation observed between ancient and modern *Meq* genes, ancient MDV genotypes could have been incapable of driving lymphoid cell transformation. To test this hypothesis experimentally, we assessed whether ancient Meq had lower transactivation capabilities, compared with modern strains, in a cultured cell–based assay.

To do so, we synthesized an ancient *Meq* gene on the basis of our highest-coverage ancient sample (OL1385; Buda Castle, Hungary; 1802 calibrated CE) and experimentally tested its transactivation function. We also cloned "very virulent" modern pathotype strains (RB1B and Md5), which each differ from ancient Meq at 13 to 14 amino acid positions (Fig. 3C and table S9). All the Meq proteins were expressed in cells alongside a chicken protein (c-Jun), with which Meq forms a heterodimer, and a luciferase reporter containing the Meq binding (AP-1) sequence.

Relative to the baseline signal, the transactivation of the very virulent Meq strains RB1B and Md5 were 7.5 and 10 times greater, respectively (Fig. 3D). Consistent with previous reports (*23*), removal of the partner protein, c-Jun, from RB1B resulted in severe abrogation of the transactivation capability (Fig. 3D). Ancient Meq exhibited a ~2.5-fold increase in transactivation relative to the baseline but was substantially lower (67 to 75%) than that of Meq from the two very virulent pathotypes (Fig. 3D). The ancient Meq was thus a demonstrably weaker transactivator than Meq from modern strains of MDV.

Given that the transcriptional regulation of target genes (both host and virus) by *Meq* is directly related to oncogenicity (*20*, *23*), the weaker transactivation we demonstrate is likely associated with reduced or absent tumor formation. These data indicate that ancient MDV strains were unlikely to cause tumors and were less pathogenic than modern strains. Ancient MDV likely established a chronic infection

characterized by slower viral replication, low levels of viral shedding, and low clinical pathology, which facilitated maximal lifetime viral transmission in preindustrialized, low-density settings.

Conclusions

Overall, our results demonstrate that MDV has been circulating in western Eurasia for at least the past millennium. By reconstructing and functionally assessing ancient and modern genomes, we showed that ancient MDV strains were likely substantially less virulent than modern strains and that the increase in virulence took place over the past century. Along with changes in several known virulence factors, we identified sequence changes in the *Meq* gene—the master regulator of oncogenesis—that drove its enhanced ability to transactivate its target genes and drive tumor formation. The historical perspective that our results provide can form the basis on which to rationally improve modern vaccines and track or even predict future virulence changes. Last, our results highlight the utility of functional paleogenomics to generate insights into the evolution and fundamental biological workings of pathogen virulence.

REFERENCES AND NOTES

1. J. Marek, *Dtsch. Tierarztl. Wochenschr.* **15**, 417–421 (1907).
2. C. Morrow, F. Fehler, in *Marek's Disease*, F. Davison, V. Nair, Eds. (Academic Press, 2004), pp. 49–61.
3. A. F. Read *et al*., *PLOS Biol.* **13**, e1002198 (2015).
4. C. S. Eidson, K. W. Washburn, S. C. Schmittle, *Poult. Sci.* **47**, 1646–1648 (1968).
5. N. Osterrieder, J. P. Kamil, D. Schumacher, B. K. Tischer, S. Trapp, *Nat. Rev. Microbiol.* **4**, 283–294 (2006).
6. E. A. Dimopoulos *et al*., *PLOS Comput. Biol.* **18**, e1010493 (2022).
7. J. Trimpert *et al*., *Evol. Appl.* **10**, 1091–1101 (2017).
8. A. J. Drummond, M. A. Suchard, D. Xie, A. Rambaut, *Mol. Biol. Evol.* **29**, 1969–1973 (2012).
9. K. Li *et al*., *Front. Microbiol.* **13**, 1046832 (2022).
10. K. Majander *et al*., *Curr. Biol.* **30**, 3788–3803.e10 (2020).
11. B. Mühlemann *et al*., *Science* **369**, eaaw8977 (2020).
12. M. Teng *et al*., *J. Gen. Virol.* **96**, 637–649 (2015).
13. Z. Yang, *Mol. Biol. Evol.* **24**, 1586–1591 (2007).
14. Y. Benjamini, Y. Hochberg, *J. R. Stat. Soc.* **57**, 289–300 (1995).
15. A. R. Omar, K. A. Schat, *Virology* **222**, 87–99 (1996).
16. C. J. Markowski-Grimsrud, K. A. Schat, *Vet. Immunol. Immunopathol.* **90**, 133–144 (2002).
17. S. Halabi *et al*., *PLOS Biol.* **19**, e3001057 (2021).
18. S. Haertle *et al*., *Front. Microbiol.* **8**, 2543 (2017).
19. A. T. Engel, R. K. Selvaraj, J. P. Kamil, N. Osterrieder, B. B. Kaufer, *J. Virol.* **86**, 8536–8545 (2012).
20. B. Lupiani *et al*., *Proc. Natl. Acad. Sci. U.S.A.* **101**, 11815–11820 (2004).
21. A. M. Conradie *et al*., *PLOS Pathog.* **16**, e1009104 (2020).
22. K. G. Renz *et al*., *Avian Pathol.* **41**, 161–176 (2012).
23. Z. Qian, P. Brunovskis, F. Rauscher 3rd, L. Lee, H. J. Kung, *J. Virol.* **69**, 4037–4044 (1995).
24. Materials and methods are available as supplementary materials.
25. S. R. Fiddaman *et al*., antonisdim, antonisdim/MDV: ancient MDV version 1.0.1, Zenodo (2023); doi:10.5281/zenodo.10022436.

ACKNOWLEDGMENTS

This research used the University of Oxford's Advanced Research Computing, Queen Mary's Apocrita, and the Leibniz-Rechenzentrum (LRZ) High Performance Computing facility. **Funding:** This work was supported by the European Research Council (grants ERC-2019-StG-853272-PALAEOFARM or ERC-2013-StG-337574-UNDEAD or both to S.R.F., L.A.F.F., G.L., and A.L.S.); Wellcome Trust (grant 210119/Z/18/Z to S.R.F. and L.A.F.F.); the Oxford Martin School Pandemic Genomics Programme (to S.R.F., L.d.P., and O.G.P.); AHRC (grant AH/L006979/1 to G.L., O.L., and N.S.); European Union's Horizon 2020 research and innovation program under the Marie Sklodowska-Curie (grant agreement 895107 to O.L.); BBSRC (grant BB/M011224/1 to S.D.); and Postdoctoral grant 12U7121N of the Research Foundation–Flanders (Fonds voor Wetenschappelijk Onderzoek) (to B.V.). **Author contributions:** Conceptualization: S.R.F., A.L.S., L.A.F.F., and G.L. Methodology: S.R.F., E.A.D., A.L.S., L.A.F.F., G.L., B.V., L.d.P., V.N., O.L., and O.G.P. Sample provision: O.L., N.M., G.F., R.S., H.B., L.D.-S., D.N.S., I.V.A., O.P., M.S., H.D., H.F., A.S.M., A.A.V., A.F., N.S., J.B., A.O.A., O.V.A., M.M., L.Z., and V.N. Investigation: S.R.F., E.A.D., O.L., L.d.P., B.V., S.C., A.F.H., K.T., P.G.F., S.D., H.L., G.C.B., O.G.P., V.N., G.L., A.L.S., and L.A.F.F. Visualization: S.R.F. Funding acquisition: L.A.F.F., A.L.S., and G.L. Project administration: S.R.F., L.A.F.F., A.L.S., and G.L. Supervision: L.A.F.F., A.L.S., and G.L. Writing – original draft: S.R.F., L.A.F.F., A.L.S., and G.L. Writing – review and editing: S.R.F., E.A.D., O.L., L.d.P., B.V., S.C., A.F.H., K.T., P.G.F., S.D., N.M., H.L., G.F., R.S., H.B., L.D.-S., D.N.S., I.V.A., O.P., M.S., H.D., H.F., A.S.M., A.A.V., A.F., N.S., G.C.B., J.B., A.O.A., O.V.A., M.M., O.G.P., V.N., G.L., A.L.S., and L.A.F.F. **Competing interests:** The authors declare that they have no competing interests. **Data and materials availability:** All MDV sequence data generated have been deposited in GenBank under accession PRJEB64489. Code is available at GitHub (https://github.com/antonisdim/MDV) and archived at Zenodo (https://zenodo.org/records/10022436) (*25*).

SUPPLEMENTARY MATERIALS

science.org/doi/10.1126/science.adg2238
Materials and Methods
Supplementary Text
Figs. S1 to S9
Tables S1 to S13
References (*26*–*74*)
MDAR Reproducibility Checklist

Submitted 22 December 2022; resubmitted 15 March 2023
Accepted 25 October 2023
10.1126/science.adg2238